

# $Z \rightarrow \tau\tau$ and $W \rightarrow \tau\nu_\tau$ Cross-Sections at the LHC

Philip Ilten

on behalf of the LHCb Collaboration  
including results from ATLAS and CMS

*School of Physics, University College Dublin*

---

## Abstract

Measurements of the  $Z \rightarrow \tau\tau$  and  $W \rightarrow \tau\nu_\tau$  cross-sections at the LHC with data taken at  $\sqrt{s} = 7$  TeV are reported for the ATLAS, CMS, and LHCb experiments. All results are found to agree with the Standard Model.

*Keywords:* LHC, ATLAS, CMS, LHCb, electroweak, tau production

---

## 1. Introduction

The production of  $Z$  and  $W$  bosons from  $pp$ -collisions, and their subsequent decays to  $\tau$ -leptons at the Large Hadron Collider (LHC) not only provides important tests of the Standard Model (SM), but also lays the groundwork for the study of beyond the SM physics using  $\tau$ -lepton signatures.

Decays of  $Z$  bosons to  $\tau$ -lepton pairs are both a mechanism for experimentally measuring hadronic  $\tau$ -lepton identification efficiencies [1, 2] and a calibration channel for neutral Higgs searches [3, 4]. The final states of  $\tau$ -leptons produced from  $W$  bosons can be used to measure the polarization of the  $W$  [5] boson or to search for charged Higgses [6, 7].

In this review, the complete set of  $Z \rightarrow \tau\tau$  and  $W \rightarrow \tau\nu_\tau$  cross-sections, as measured by the ATLAS, CMS, and LHCb experiments on the LHC, are reported using 2010 and 2011 datasets taken at  $\sqrt{s} = 7$  TeV. A full summary of the results, including corresponding references, is provided in Table 1, and a comparison of the theoretical agreement of the results is given in Figure 1.

All three detectors are fully instrumented with charged particle trackers, electromagnetic and hadronic calorimeters, and muon systems. Both ATLAS [8] and CMS [9] are general purpose detectors designed to cover a central pseudorapidity range of  $|\eta| < 2.4$ , while the LHCb [10] detector is a forward arm spectrometer, purpose built for  $B$ -hadron physics, covering the forward pseudorapidity range  $2.0 < \eta < 5.0$ .

## 2. $Z \rightarrow \tau\tau$

Four final states produced from the  $\tau$ -lepton decays of  $Z \rightarrow \tau\tau$  events are considered by all three experiments: two muons ( $\tau_\mu\tau_\mu$ ), a muon and an electron ( $\tau_\mu\tau_e$ ), a muon and a hadronic jet ( $\tau_\mu\tau_h$ ), and an electron and a hadronic jet ( $\tau_e\tau_h$ ). Six backgrounds to these final states are considered: Drell-Yan production of di-muon or di-electron pairs,  $WW$  decays,  $t\bar{t}$  decays,  $Z$  production with an associated jet,  $W$  production with an associated jet, and QCD multijet events.

### 2.1. Particle Selection

All final states are triggered by a muon with a  $p_T$  greater than 9 – 15 GeV, except the  $\tau_e\tau_h$  final state, which is triggered by an electron with  $E_T$  greater than 12 – 15 GeV for ATLAS and CMS and  $p_T$  greater than 10 GeV for LHCb. An additional hadronic trigger is included by ATLAS for the  $\tau_e\tau_h$  final state, while the LHCb  $\tau_\mu\tau_e$  final state is split into a muon triggered final state ( $\tau_\mu\tau_e$ ), and an electron and muon triggered final state ( $\tau_e\tau_\mu$ ).

Muons are identified by requiring an isolated track associated with muon system hits. Electrons are identified by requiring an isolated track associated with electromagnetic calorimeter energy. Both one and three-pronged hadronic  $\tau$ -lepton decays are identified within ATLAS and CMS using the anti- $k_T$  jet algorithm and requiring one or three charged particles, whereas only single-pronged hadronic  $\tau$ -lepton decays are identified within LHCb by requiring a single isolated track with an associated hadronic calorimeter energy and minimal electromagnetic calorimeter energy.

Exp.	Analysis	$N_{\text{obs}}$	$N_{\text{bkg}}$	$\sigma \pm \text{stat.} \pm \text{syst.} \pm \text{lumi.}$	$\mathcal{L}$	Data	Ref.	
ATLAS	$Z \rightarrow$	$\tau_\mu\tau_\mu$	90	47	$0.96 \pm 0.22 \pm 0.12 \pm 0.03$ nb	36 pb <sup>-1</sup>	2010	[11]
		$\tau_\mu\tau_e$	1035	56	$0.96 \pm 0.03 \pm 0.09 \pm 0.04$ nb	1.55 fb <sup>-1</sup>		
		$\tau_\mu\tau_h$	5184	793	$0.91 \pm 0.01 \pm 0.09 \pm 0.03$ nb	1.55 fb <sup>-1</sup>	2011	[12]
		$\tau_e\tau_h$	2600	449	$1.00 \pm 0.02 \pm 0.13 \pm 0.04$ nb	1.34 fb <sup>-1</sup>		
	$W \rightarrow$	$\tau_h\nu_\tau$	2335	411	$11.1 \pm 0.3 \pm 1.7 \pm 0.4$ nb	34 pb <sup>-1</sup>	2010	[13]
CMS	$Z \rightarrow$	$\tau_\mu\tau_\mu$	58	23	$1.14 \pm 0.27 \pm 0.04 \pm 0.05$ nb			
		$\tau_\mu\tau_e$	101	14	$0.99 \pm 0.12 \pm 0.06 \pm 0.04$ nb	36 pb <sup>-1</sup>	2010	[14]
		$\tau_\mu\tau_h$	517	228	$0.83 \pm 0.07 \pm 0.19 \pm 0.03$ nb			
		$\tau_e\tau_h$	540	346	$0.94 \pm 0.11 \pm 0.22 \pm 0.04$ nb			
	$W \rightarrow$	$\tau_h\nu_\tau$	372	155	<i>not measured</i>	18 pb <sup>-1</sup>	2010	[15]
LHCb	$Z \rightarrow$	$\tau_\mu\tau_\mu$	124	42	$77.4 \pm 10.4 \pm 8.6 \pm 2.7$ pb	1.03 fb <sup>-1</sup>		
		$\tau_\mu\tau_e$	421	130	$75.2 \pm 5.4 \pm 4.1 \pm 2.6$ pb	1.03 fb <sup>-1</sup>		
		$\tau_e\tau_\mu$	155	57	$64.2 \pm 8.2 \pm 4.9 \pm 2.2$ pb	0.96 fb <sup>-1</sup>	2011	[16]
		$\tau_\mu\tau_h$	189	53	$68.3 \pm 7.0 \pm 2.6 \pm 2.4$ pb	1.03 fb <sup>-1</sup>		
		$\tau_e\tau_h$	101	37	$77.9 \pm 12.2 \pm 6.1 \pm 2.7$ pb	0.96 fb <sup>-1</sup>		

Table 1: A complete summary of the individual  $Z \rightarrow \tau\tau$  and  $W \rightarrow \tau\nu_\tau$  cross-section analyses of ATLAS, CMS, and LHCb using 2010 and 2011 datasets. The experiment, final state, number of observed events ( $N_{\text{obs}}$ ), number of background events ( $N_{\text{bkg}}$ ), cross-section measurement ( $\sigma$ ), integrated luminosity ( $\mathcal{L}$ ), dataset, and reference are given for each analysis.

## 2.2. Event Selection

The  $Z \rightarrow \tau\tau$  signal produces a high mass back-to-back final state in the transverse plane with missing energy ( $\cancel{E}_T$ ) and a  $p_T$  imbalance between the two  $\tau$ -lepton decay products due to unreconstructed neutrinos. Additionally, the lifetime of the  $\tau$ -lepton produces decay products with an enhanced impact parameter. Selection requirements based on these five signatures are used by the three experiments to separate signal from background.

For ATLAS, a visible mass selection requirement is placed on all four final states, and a transverse mass requirement on the  $\tau_\mu\tau_h$  and  $\tau_e\tau_h$  final states. A requirement on the transverse separation of the  $\tau$ -lepton decay products and the  $\cancel{E}_T$  of the event is used for all final states except  $\tau_\mu\tau_\mu$ , where further requirements on the angular separation,  $p_T$  asymmetry, and impact parameters of the two  $\tau$ -lepton decay products are applied.

For CMS, only a transverse mass requirement is applied to the  $\tau_\mu\tau_e$ ,  $\tau_\mu\tau_h$ , and  $\tau_e\tau_h$  final states. Due to the large Drell-Yan background to the  $\tau_\mu\tau_\mu$  final state, requirements are placed on the visible mass, transverse separation between the muons and  $\cancel{E}_T$ , the muon  $p_T$  asymmetry, and the impact parameter of the muons.

Unlike for ATLAS and CMS, missing energy cannot be measured within LHCb. However, a high resolution vertex locator allows for strict requirements to be placed on the  $\tau$ -lepton decay product impact parameters for the  $\tau_\mu\tau_\mu$ ,  $\tau_\mu\tau_h$ , and  $\tau_e\tau_h$  final states. Both a visible mass and

transverse separation requirement is placed on all final states, while an additional  $p_T$  asymmetry requirement is also placed on the  $\tau_\mu\tau_\mu$  final state.

## 2.3. Background Estimation

Drell-Yan production of lepton pairs is the primary background to the  $\tau_\mu\tau_\mu$  final state for all three experiments, as well as the  $\tau_e\tau_h$  final state for ATLAS and CMS. The Drell-Yan visible mass shape is determined for ATLAS from simulation, while for both CMS and LHCb the template is obtained with a reversed impact parameter requirement. For ATLAS and LHCb the template is normalized to the on-shell Z mass peak, and for CMS normalized to an impact parameter side-band.

The QCD multijet background is large in the  $\tau_\mu\tau_h$  and  $\tau_e\tau_h$  final states, and a visible mass shape is determined from data for all three experiments by requiring candidates with same-sign charge. The normalization is also taken from data, scaling the number of same-sign events by the estimated opposite-sign/same-sign event ratio for the background.

The  $W$  with jets background mass shape is determined from simulation for all three experiments and normalized using transverse mass side-bands for ATLAS and CMS, and a same-sign side-band for LHCb. The  $Z$  with jets visible mass shape is taken from simulation for ATLAS and LHCb, and from a reversed impact parameter requirement for CMS. The background is normalized using a visible mass side-band for AT-

LAS, an impact parameter side-band for CMS, and a same-sign side-band for LHCb.

For all three experiments the visible mass distributions for the  $WW$  and  $t\bar{t}$  backgrounds are estimated from simulation. The normalization for these backgrounds is also taken from simulation for ATLAS and LHCb, and from a transverse mass side-band for CMS. Both the  $WW$  and  $t\bar{t}$  background contributions are minimal for all final states.

#### 2.4. Systematics

For both ATLAS and CMS the hadronic  $\tau$ -lepton identification efficiency and energy scale is the primary systematic uncertainty for the  $\tau_\mu\tau_h$  and  $\tau_e\tau_h$  final states, ranging from 8% – 23%. In the  $\tau_\mu\tau_\mu$  final state the primary uncertainty is between 2% – 9% from muon efficiency and acceptance, and for the  $\tau_\mu\tau_e$  final state is between 2% – 6% from electron efficiency.

For LHCb, the Drell-Yan background provides the largest systematic uncertainty of 8% to the  $\tau_\mu\tau_\mu$  final state. Electron reconstruction efficiency contributes the primary uncertainty to the  $\tau_\mu\tau_e$ ,  $\tau_e\tau_\mu$ , and  $\tau_e\tau_h$  final states of 4%, while the impact parameter selection efficiency provides a 2% uncertainty to the  $\tau_\mu\tau_h$  final state.

#### 2.5. Results

The measured cross-section, number of observed events, and number of background events for each final state of all three experiments is given in Table 1. Note the reduced statistics of the LHCb results, due to the acceptance of the detector, but the enhanced purity of the  $\tau_\mu\tau_\mu$  final state.

The combined  $Z \rightarrow \tau\tau$  cross-section measurement for each experiment is given in Table 2, including the fiducial definition and predicted theory result. The ATLAS and CMS theory predictions were calculated using FEWZ [17], while the LHCb prediction was calculated with DYNLLO [18]. The ATLAS combined result does not include the  $\tau_\mu\tau_\mu$  final state.

### 3. $W \rightarrow \tau\nu_\tau$

Due to the large  $W \rightarrow \ell\nu_\ell$  background to leptonically decaying  $\tau$ -leptons produced from  $W$  bosons, only hadronic decays of the  $\tau$ -lepton are considered for the ATLAS and CMS  $W \rightarrow \tau\nu_\tau$  analyses. QCD jets,  $W \rightarrow \ell\nu_\ell$ ,  $W \rightarrow \tau_\ell\nu_\tau$ , and  $Z$  with jets events provide the primary backgrounds to this signal. Of the three experiments, only ATLAS has performed a  $W \rightarrow \tau\nu_\tau$  measurement. An observation has been made with CMS, but without a cross-section measurement.

Exp.	$\sigma \pm \text{stat.} \pm \text{syst.} \pm \text{lumi.}$	$\sigma$ theory
ATLAS	$0.92 \pm 0.02 \pm 0.08 \pm 0.03$ nb $66 < M_{\tau\tau} < 116$ GeV	$0.96 \pm 0.05$ nb FEWZ
CMS	$1.00 \pm 0.05 \pm 0.08 \pm 0.04$ nb $60 < M_{\tau\tau} < 120$ GeV	$0.97 \pm 0.04$ nb FEWZ
LHCb	$71.4 \pm 3.5 \pm 2.8 \pm 2.5$ pb $p_T^\tau > 20$ GeV, $2.0 < \eta^\tau < 4.5$ $60 < M_{\tau\tau} < 120$ GeV	$74.3 \pm 2.1$ pb DYNLLO

Table 2: Combined  $Z \rightarrow \tau\tau$  and theoretical cross-section results for the three experiments. The ATLAS result does not include the  $\tau_\mu\tau_\mu$  final state.

#### 3.1. Particle Selection

A  $p_T > 12$  GeV trigger on the hadronic  $\tau$ -lepton combined with a  $\cancel{E}_T > 20$  GeV trigger is used to select events for ATLAS, while a  $p_T > 20$  GeV hadronic  $\tau$ -lepton trigger and  $\cancel{E}_T > 25$  GeV trigger is used for CMS.

Hadronic  $\tau$ -leptons are selected for ATLAS using a boosted decision tree based on the collimation, impact parameter, and lead track  $p_T$  over electromagnetic calorimeter energy of the hadronic  $\tau$ -lepton candidate. For the CMS selection, requirements are placed on the hadronic  $\tau$ -lepton lead track  $p_T$ , isolation, and associated muon hits.

#### 3.2. Event Selection

To eliminate  $W$  and  $Z$  with jets backgrounds, events with high  $p_T$  leptons outside the hadronic  $\tau$ -lepton jet are rejected for both ATLAS and CMS. A large  $\cancel{E}_T$  is also required for both to reduce the QCD jet background. Additionally, a high  $\cancel{E}_T$  significance and transverse separation between the  $\tau$ -lepton and  $\cancel{E}_T$  is required for ATLAS, while the ratio of the  $\tau$ -lepton jet  $p_T$  to the  $p_T$  of the remaining jets is required to be large for CMS.

#### 3.3. Background Estimation

The  $W$  and  $Z$  background transverse mass shapes for both ATLAS and CMS are determined and normalized using simulation. The QCD jet background transverse mass shape and normalization is determined using an ABCD method for both. For ATLAS, requirements are made on the  $\cancel{E}_T$  significance and hadronic  $\tau$ -lepton identification, while requirements on the  $\cancel{E}_T$  and ratio of  $\tau$ -lepton jet  $p_T$  to the  $p_T$  of the remaining jets are used for CMS.

### 3.4. Systematics

The primary systematic uncertainty for the ATLAS  $W \rightarrow \tau_h \nu_\tau$  cross-section measurement is due to the identification efficiency for the hadronic  $\tau$ -lepton jets and estimated to be 10%. For CMS, no cross-section measurement was made, and so no uncertainty analysis is available.

### 3.5. Results

The number of observed  $W \rightarrow \tau \nu_\tau$  events and background events is given in Table 1 for both ATLAS and CMS, as well as the measured ATLAS cross-section. To determine the total cross-section, the ATLAS  $W \rightarrow \tau_h \nu_\tau$  cross-section is extrapolated from the measured fiducial region to full acceptance, and divided by the experimentally known branching fraction for  $\tau$ -leptons to hadrons. The result given in Table 1 agrees well with the theoretically predicted value of  $10.5 \pm 0.5$  nb calculated using FEWZ.

## 4. Conclusion

A comparison of the measured cross-sections of Table 1 and Table 2 divided by their predicted theoretical values is given in Figure 1. The red points represent the combined results and the black points individual final states. The dark error bars correspond to statistical uncertainty, while the light error bars correspond to the combined systematic uncertainty and uncertainty due to the integrated luminosity. The dark yellow band indicates the theoretical uncertainty of the prediction.

There is good agreement between all measured cross-sections and their theoretical values. Currently, ATLAS provides the most statistics for the combined  $Z \rightarrow \tau\tau$  cross-section measurement, while LHCb yields the most precise cross-section measurement. The ATLAS  $W \rightarrow \tau \nu_\tau$  measurement has a large systematic uncertainty and does not allow for a more precise test of the  $W \rightarrow \tau \nu_\tau$  to  $W \rightarrow \mu \nu_\mu$  ratio measured at LEP.

## References

- [1] ATLAS Collab., Tech. Rep. ATLAS-CONF-2011-152 (2011).
- [2] CMS Collab., JINST 7 (2012) P01001. [arXiv:1109.6034](#).
- [3] ATLAS Collab., Tech. Rep. ATLAS-CONF-2012-094 (2012).
- [4] CMS Collab., Phys.Lett. B713 (2012) 68–90. [arXiv:1202.4083](#).
- [5] ATLAS Collab., Eur.Phys.J. C72 (2012) 2062. [arXiv:1204.6720](#).
- [6] ATLAS Collab., JHEP 1206 (2012) 039. [arXiv:1204.2760](#).
- [7] CMS Collab., JHEP 1207 (2012) 143. [arXiv:1205.5736](#).
- [8] ATLAS Collab., JINST 3 (2008) S08003.

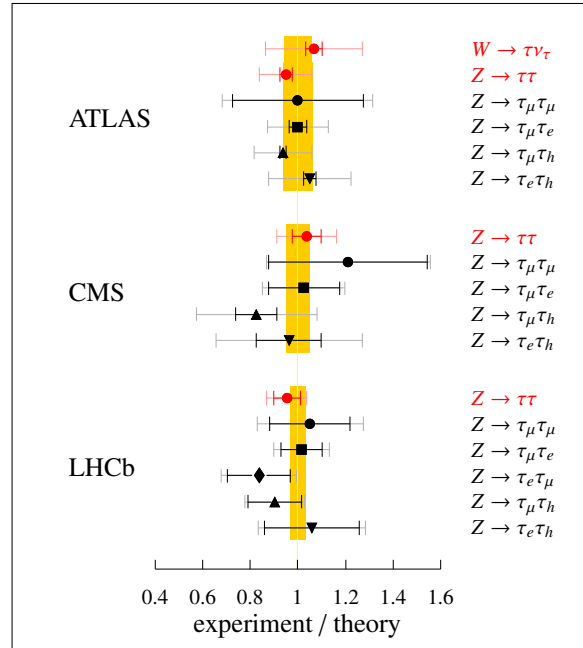


Figure 1: Ratios of the experimental cross-section measurements of Table 1 and Table 2 to their expected theoretical values. The combined results are given in red and the individual final states in black. The dark error bars are the statistical uncertainty, while the light error bars are the combined systematic uncertainty and uncertainty due to the integrated luminosity. The dark yellow band indicates the theoretical uncertainty centered about the light yellow line.

- [9] CMS Collab., JINST 3 (2008) S08004.
- [10] LHCb Collab., JINST 3 (2008) S08005.
- [11] ATLAS Collab., Phys.Rev. D84 (2011) 112006. [arXiv:1108.2016](#).
- [12] ATLAS Collab., Tech. Rep. ATLAS-CONF-2012-006 (2012).
- [13] ATLAS Collab., Phys.Lett. B706 (2012) 276–294. [arXiv:1108.4101](#).
- [14] CMS Collab., JHEP 1108 (2011) 117. [arXiv:1104.1617](#).
- [15] CMS Collab., Tech. Rep. CMS-PAS-EWK-11-002 (2011).
- [16] LHCb Collab., [arXiv:1210.6289](#).
- [17] R. Gavin, Y. Li, F. Petriello, S. Quackenbush, Comput.Phys.Commun. 182 (2011) 2388–2403. [arXiv:1011.3540](#).
- [18] S. Catani, M. Grazzini, Phys.Rev.Lett. 98 (2007) 222002. [arXiv:hep-ph/0703012](#).